Modified Data-Pilot-Multiplexed Schemes for OFDM Systems

Xiaoyu Fu, *Student Member, IEEE*, and Hlaing Minn, *Member, IEEE*

***Abstract*— In data-pilot-multiplexed OFDM schemes, data-interference to pilot tones causes degradation in frequency offset and channel estimation. This paper derives the best data-pilot-multiplexed scheme in terms of minimizing data-interference on pilot tones. This design gives a correlated data insertion scheme (CD) (data on the left and right adjacent tones of each pilot are correlated) and a null data insertion scheme (ND) (no data are transmitted on the left and right adjacent tones of each pilot). Both schemes outperform conventional data-pilot-multiplexed schemes (CV) significantly (over 7 dB SNR advantage at the uncoded BER of 2×10^{-2} and pilot-to-data energy ratio (PDER) of 5 dB). With the BLUE frequency offset estimator, the CD scheme yields a better performance than the ND scheme while having a slight advantage in data throughput. A modified CD scheme is also presented which transmits the same data rate at similar complexity as the CV scheme does while achieving a significant BER improvement (over 3 dB SNR advantage at the uncoded BER of 2×10^{-2} and PDER of 5 dB).**

***Index Terms*— Data-pilot-multiplexed scheme, frequency offset, inter-carrier interference, OFDM.**

I. Introduction

OFDM is very sensitive to frequency offsets which destroy orthogonality among sub-carriers, introduce inter-carrier interference (ICI) and can degrade the error performance significantly. Mainly two approaches have been proposed in the literature to counteract the frequency offset effect. The first approach employs a highly accurate frequency offset estimator by which it compensates for the ICI effect and/or corrects the local carrier frequency. Training preamble-based estimators (e.g., [1]-[3]) enjoy high accuracy, low complexity, and low delay at the expense of training overhead while semi-blind or blind estimators (e.g., [4]-[6]) save training overhead at the expense of high complexity, long delay, and/or less robust/accurate estimation. The second approach (e.g., [7]-[8]) utilizes a self-ICI-cancellation scheme where data redundancy (at a code rate of 1/2 or smaller) in frequency domain is introduced such that significant ICI terms are almost cancelled out. In most of the consumer-related wireless systems, a data rate sacrifice is not desirable and hence, the first approach is typically adopted. For achieving reliable performance with low complexity at the receiver, all existing OFDM-based wireless systems transmit data-pilot-multiplexed OFDM symbols at a regular rate in order to track the variations in channel gains and synchronization parameters.

The existing low-complexity, high-accuracy frequency offset estimators such as [1]-[3] were developed based on training signal only. Their performance/applicability for data-pilot-multiplexed scheme needs further investigation which is pursued in this paper. Consider an OFDM symbol of N sub-carriers consisting of N_p pilot tones and N_d data tones. If no processing is performed on data tones, the data throughput[1] is N_d/N but the frequency offset and channel estimation performance would be degraded due to data-interference. If zero interference is desired for the estimation, all N_d data tones have to be nulled and the data throughput would be zero. If self-ICI-cancellation code of rate 1/2 is applied for data tones in order to reduce data-interference to pilot, the data throughput would be $N_d/(2N)$ and this amount of throughput loss is undesirable.

In an attempt to improve the estimation performance while keeping data throughput high, we consider modified data-pilot-multiplexed schemes where left and right adjacent data tones of each pilot are modified. The corresponding data throughput range is from $(N_d - 2N_p)/N$ (where all adjacent data tones are nulled) to N_d/N (where no modification/processing is performed on adjacent data tones, i.e., conventional data-pilot-multiplexed scheme (CV)). The data throughputs of our considered schemes are much larger than that of self-ICI-cancellation code. By minimizing the interferences of adjacent data tones on pilot tones, we obtain two schemes (null data insertion scheme (ND) and correlated data insertion scheme (CD)) which give quite appreciable improvement in estimation and BER performance over the CV scheme.

II. Signal Model

Consider a data-pilot-multiplexed OFDM symbol consisting of N sub-carriers. The indices of all sub-carriers[2] are denoted by the set $\mathcal{J}$ and those of N_p pilot tones, N_d data tones, and N_n null tones are denoted by the disjoint sets $\mathcal{J}_p$, $\mathcal{J}_d$, and $\mathcal{J}_n$, respectively, where $\mathcal{J}_p \bigcup \mathcal{J}_d \bigcup \mathcal{J}_n = \mathcal{J}$ and $N_p+N_d+N_n = N$. Since cyclically-equi-spaced, equi-energy pilot tones are optimal for channel estimation [9] and they are also used in low-complexity, high-accuracy frequency offset estimators such as [2]-[3], we adopt cyclically-equi-spaced,

Manuscript received June 15, 2005; revised January 24, 2006; accepted April 7, 2006. The associate editor coordinating the review of this paper and approving it for publication was C. Tellambura. This work was supported in part by the Erik Jonsson School Research Excellence Initiative, the University of Texas at Dallas. This paper was presented in part at IEEE VTC 2005 (Fall) conference.

The authors are with the Department of Electrical Engineering, University of Texas at Dallas, P. O. Box 830688, EC 33, Richardson, TX 75083-0688 USA (e-mail: xxf031000@utdallas.edu; hlaing.minn@utdallas.edu).

Digital Object Identifier 10.1109/TWC.2007.05428.

[1]In this paper, the data throughput is defined as the ratio of the number of information-bearing data sub-carriers to the total number of OFDM sub-carriers for the comparison of different data-pilot-multiplexed schemes.

[2]In this paper, the sub-carrier index refers to the FFT index, not the transmitted tone index in the frequency-domain.

equi-energy N_p pilot tones multiplexed with N_d data tones, but our proposed approaches described in Section III can be applied to other pilot schemes as well. For the pilot tone spacing of $D = N/N_p$ and $\mathcal{J}=\{0, 1, \ldots, N-1\}$, we have $\mathcal{J}_p = \{l + mD \ : \ m = 0, \ldots, N_p - 1\}$ where $l \in \{0, \ldots, D-1\}$. $\mathcal{J}_d$ can be separated into two disjoint sets $\mathcal{J}_{d,a}$ and $\mathcal{J}_{d,b}$ where $\mathcal{J}_{d,a} = \{l + mD \pm 1 \ : \ m = 0, \ldots, N_p - 1\}$ corresponds to data tones adjacent to pilot tones and $\mathcal{J}_{d,b}$ corresponds to the remaining data tones. We denote the set $\mathcal{J}_{p,a}$ as the indices of the pilot tones which have data tones at both their left and right adjacent tones.

A multi-path fading channel with L sample-spaced taps is considered and the tap gains $\boldsymbol{h} = \{h_l : \ l = 0, \ldots, L-1\}$ are assumed to remain constant over one OFDM symbol. The low-pass equivalent received sample after the cyclic prefix removal is given by

$$y_n = \frac{1}{N} \ e^{\frac{j2\pi nv}{N}} \sum_{l=0}^{L-1} h_l \sum_{k=0}^{N-1} C_k e^{\frac{j2\pi(n-l)k}{N}} + w_n \tag{1}$$

where v is a normalized frequency offset[3] introduced by oscillators' inaccuracies and $\{w_n\}$ are independent and identically distributed, circularly-symmetric zero-mean complex Gaussian noise samples with variance $E[|w_n|^2] = \sigma^2$. C_k is the k-th sub-carrier symbol defined by

$$C_k = \begin{cases} P_k, & k \in \mathcal{J}_p \\ S_k, & k \in \mathcal{J}_d \\ 0, & \text{otherwise} \end{cases} \tag{2}$$

where $\{P_k\}$, which are non-zeros only at $k \in \mathcal{J}_p$, represent pilot tones, and $\{S_k\}$, which are non-zeros only at $k \in \mathcal{J}_d$, represent data tones. After FFT operation, the received k-th sub-carrier symbol is given by

$$Y_k = I_0 C_k H_k + \sum_{n=0, n\neq k}^{N-1} I_{n-k} C_n H_n + W_k \equiv I_0 C_k H_k + G_k + W_k \tag{3}$$

where H_k is the k-th sub-carrier frequency response, $\{W_k\}$ are frequency-domain Gaussian noise samples corresponding to the time-domain noise samples $\{w_n\}$, I_{n-k} is the ICI coefficient corresponding to the interference from n-th tone to k-th tone and given by

$$I_{n-k} = \frac{1}{N} \sum_{m=0}^{N-1} e^{\frac{j2\pi(v+n-k)m}{N}} \tag{4}$$

and I_0 is the self-distortion coefficient of each sub-carrier due to the frequency offset. In (3), G_k represents the total interference experienced at the k-th sub-carrier. The amplitudes of the ICI coefficients are shown in Fig. 1(a) for an OFDM system with $N = 256$. It can be observed that the interferences coming from nearer sub-carriers are larger.

III. Proposed Data-Pilot-Multiplexed Schemes

Let us consider the symbol error probability of a pilot-data-multiplexed scheme. The receiver performs frequency offset estimation and compensation, and then channel estimation, equalization, and detection. The statistics of the normalized

[3] It is a frequency offset divided by the sub-carrier spacing. We assume that $|v| < D/2$.

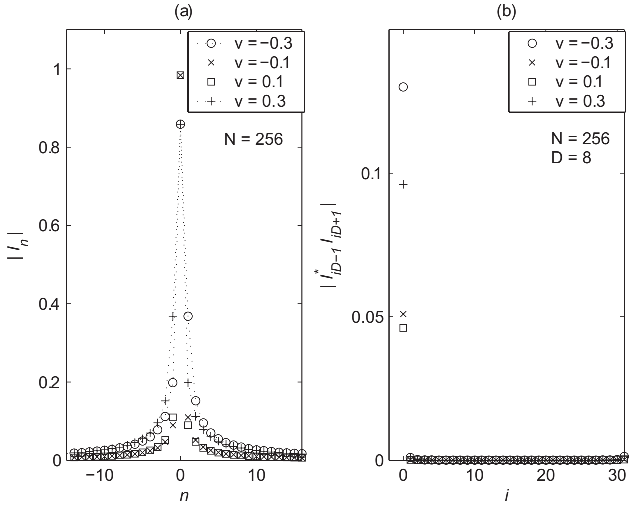

Fig. 1. (a) The amplitudes of the ICI coefficients, (b) The absolute values of the terms $\{I^*_{iD-1} I_{iD+1}\}$ from β (illustrating the dominant term $I^*_{-1} I_1$).

frequency offset estimate and hence the residual (after frequency offset compensation) normalized frequency offset Δv depend on the channel $\boldsymbol{h}$, the transmitted symbols $\{C_n\}$, the estimator, and the noise level. The statistics of the channel estimate depend on Δv, $\boldsymbol{h}$, $\{C_n\}$, the estimator, and the noise level. After equalization, the decision variable on the k-th sub-carrier is given by

$$Z_k = \frac{Y_k}{\hat{H}_k} = \frac{I_0 C_k H_k}{\hat{H}_k} + \frac{G_k}{\hat{H}_k} + \frac{W_k}{\hat{H}_k}. \tag{5}$$

Let $\{A_{k,i} \ : \ i = 1, \ldots, M_k\}$ be the signal constellation on the k-th sub-carrier and $\mathcal{R}_{k,i}$ be the decision region for $A_{k,i}$. Then the probability of correct symbol detection on the k-th sub-carrier given Δv, $\boldsymbol{h}$, and $\{C_n\}$ is

$$P_k(\text{correct}|\Delta v, \boldsymbol{h}, \{C_n\}) = \text{Prob}\left[Z_k \in R_{k,i}|\Delta v, \boldsymbol{h}, \{C_n\})\right]. \tag{6}$$

The symbol error probability is given by

$$\begin{aligned} P_e \ = \ & 1 - \sum_{\{C_n\}} \text{Prob}[\{C_n\}] \int\int \\ & \frac{1}{N_d} \sum_{k\in\mathcal{J}_d} P_k(\text{correct}|\Delta v, \boldsymbol{h}, \{C_n\}) \times \\ & f(\Delta v|\boldsymbol{h}, \{C_n\}) f(\boldsymbol{h}) \ d\Delta v \ d\boldsymbol{h} \end{aligned} \tag{7}$$

where $f(a)$ is the probability density function of a, the integral with respect to $\boldsymbol{h}$ is L-dimensional, and the summation is $(\sum_{k=0}^{N-1} M_k)$-dimensional. A closed form expression of P_e is intractable. Recently, a few works [10][11] addressed P_e for much simpler systems. [10] assumed an AWGN channel with a frequency offset. [11] considered a frequency-selective channel with a frequency offset and perfect channel information, but no closed-form expression was obtained.

Alternative approaches [12][13] used the variance of the interference term to obtain the error performance degradation due to the frequency offset. All these works [10]-[13] showed that a larger frequency offset causes a larger error performance degradation. In terms of our considered system, a scheme with a better error performance means a scheme with smaller estimation errors. Since we use pilot tones to estimate the frequency offset and the channel, and the data are uncorrelated with the pilot and AWGN, the data interference increases the effective noise (interference plus AWGN) level for the estimation. Then a reasonable approach for achieving a better estimation performance irrespective of the estimation method is to minimize the data interference on the pilot tones, which we pursue in this paper.

From Fig. 1(a), we observe that the left and right adjacent tones introduce the most significant interference terms. Based on this observation together with the aim of improving estimation performance at a minimal sacrifice of data-throughput, we propose to perform some processing on every left and right adjacent data of each pilot tone so that the corresponding data interference is minimized. The possible data throughput ranges from $(N_d - 2N_p)/N$ to N_d/N. For typical systems where $N_d \gg N_p$, our data throughput sacrifice is negligible if compared to the use of self-ICI-cancellation code whose maximum data throughput is $1/2$.

For a fair comparison, we keep the same total pilot energy and the same total data energy within the data-pilot-multiplexed symbol of all data-pilot multiplexed schemes. Our processing on the left and right adjacent tones of each pilot is the same as long as they are data tones. Without loss of generality, the ICI term on the pilot transmitted at k-th ($k \in \mathcal{J}_p$) sub-carrier is given by

$$G_k = \sum_{n \in \mathcal{J}_d} I_{n-k} S_n H_n + \sum_{m \in \mathcal{J}_p, m \neq k} I_{m-k} P_m H_m. \tag{8}$$

The second term in (8) is introduced by other pilot tones and is independent of data. Since we are designing adjacent data of each pilot, we only need to consider the first term defined as

$$g_k = \sum_{n = \in \mathcal{J}_{d,a}} I_{n-k} S_n H_n + \sum_{m = \in \mathcal{J}_{d,b}} I_{m-k} S_m H_m. \tag{9}$$

We assume that the data are independent except between the two data tones adjacent to each pilot. Then g_k is a random variable with zero mean and its variance is given by

$$\begin{aligned} \sigma_{g,k}^2 &= E[g_k^* g_k] \\ &= E\Bigg[\sum_{n \in \mathcal{J}_{d,a}} |I_{n-k}|^2 |S_n|^2 |H_n|^2 + \sum_{m \in \mathcal{J}_{d,b}} |I_{m-k}|^2 |S_m|^2 |H_m|^2 \\ &\quad + 2\Re\{\sum_{m \in \mathcal{J}_{p,a}} I_{m-1-k}^* I_{m+1-k} S_{m-1}^* S_{m+1} H_{m-1}^* H_{m+1}\}\Bigg]. \end{aligned} \tag{10}$$

The correlation of data in our considered system is given by

$$E[S_n^* S_m] = \begin{cases} \sigma_1^2, & n = m, n \in \mathcal{J}_{d,a} \\ \sigma_2^2, & n = m, n \in \mathcal{J}_{d,b} \\ \rho\sigma_1^2, & n = p-1,\ m = p+1,\ p \in \mathcal{J}_{p,a} \\ \rho^*\sigma_1^2, & n = p+1,\ m = p-1,\ p \in \mathcal{J}_{p,a} \\ 0 & \text{otherwise.} \end{cases} \tag{11}$$

Since we keep the total data energy E_d to be constant, σ_1^2 and σ_2^2 are related to each other as

$$\sigma_2^2 = \frac{E_d - 2N_{p,a}\sigma_1^2}{N_d - 2N_{p,a}} \tag{12}$$

where $N_{p,a}$ denotes the number of tones in the set $\mathcal{J}_{p,a}$. Using (11)(12) and assuming $E[|H_n|^2] = \sigma_H^2$ in (10) give

$$\sigma_{g,k}^2 = \gamma_k + \sigma_1^2\,[\alpha_k + \Re\{\rho\,\beta_k\}] \tag{13}$$

$$\gamma_k = \sigma_H^2 \frac{E_d}{N_d - 2N_p} \sum_{m \in \mathcal{J}_{d,b}} |I_{m-k}|^2 \tag{14}$$

$$\alpha_k = \sigma_H^2 \left[\sum_{n \in \mathcal{J}_{d,a}} \{|I_{n-k}|^2\} - \frac{2N_{p,a}}{N_d - 2N_{p,a}} \sum_{m \in \mathcal{J}_{d,b}} |I_{m-k}|^2\right] \tag{15}$$

$$\beta_k = 2 \sum_{m \in \mathcal{J}_{p,a}} I_{m-1-k}^* I_{m+1-k}\ E[H_{m-1}^* H_{m+1}]. \tag{16}$$

Then our design becomes finding ρ and σ_1^2 which minimize the total data interference on the pilot tones as

$$\{\rho^\dagger,\ \sigma_1^{2\dagger}\} = \arg\min_{\rho,\ \sigma_1^2} \{\sigma_g^2 = \sum_{k \in \mathcal{J}_p} \sigma_{g,k}^2\} \tag{17}$$

$$= \arg\min_{\rho,\ \sigma_1^2} \{\sigma_1^2\ [\sum_{k \in \mathcal{J}_p} \alpha_k + \Re\{\rho \sum_{k \in \mathcal{J}_p} \beta_k\}]\} \tag{18}$$

where the ranges[4] are $0 \le |\rho| \le 1$, $0 \le (\theta_\rho = \text{angle}\{\rho\}) < 2\pi$ and $0 \le \sigma_1^2 \le E_d/N_d$. For any σ_1^2, the minimum of σ_g^2 is obtained by

$$\rho^\dagger = -e^{-j\theta_\beta} \tag{19}$$

where θ_β = angle$\{\sum_{k \in \mathcal{J}_p} \beta_k\}$. Substituting $\rho^\dagger$ back into (18) gives the best σ_1^2 as

$$\begin{aligned} \sigma_1^{2\dagger} &= \arg\min_{\sigma_1^2} \{\sigma_1^2[\sum_{k \in \mathcal{J}_p} (\alpha_k - |\beta_k|)]\} \\ &= \begin{cases} [\sigma_1^2]_{\max} = \frac{E_d}{N_d}, & \text{if } \sum_{k \in \mathcal{J}_p} (\alpha_k - |\beta_k|) \le 0 \\ [\sigma_1^2]_{\min} = 0, & \text{otherwise} \end{cases} \end{aligned} \tag{20}$$

which corresponds to the CD scheme when $\sum_{k \in \mathcal{J}_p} (\alpha_k - |\beta_k|) \le 0$ and the ND scheme otherwise. For a small v, we have $I_{m-1-k} \simeq I_{m+1-k}$ and hence, $|\beta_k| \simeq 2\sigma_H^2 \sum_{k \in \mathcal{J}_{p,a}} |I_k|^2$. For a larger v, $|\beta_k|$ is smaller due to a larger variation between I_{m-1-k} and I_{m+1-k}. But α_k is larger for a larger v. Hence, $\sum_{k \in \mathcal{J}_p} (\alpha_k - |\beta_k|)$ increases with v. Consequently, for a given system and channel environment, $\sum_{k \in \mathcal{J}_p} (\alpha_k - |\beta_k|) \le 0$ can be viewed as the condition where the frequency offset is less than or equal to a threshold.

Fig. 2 illustrates the proposed CD and ND schemes for a system with $N = 64$, $N_p = 4$, $N_d = 48$, $N_n = 12$, $l = 8$ and $\mathcal{J}_n = \{0, \frac{N}{2} - N_n + \lfloor \frac{N_n}{2} \rfloor, \ldots, \frac{N}{2} + \lfloor \frac{N_n}{2} \rfloor - 2\}$, where $\lfloor \cdot \rfloor$ represents the floor operation. Note that the N_n null tones are located at the DC-sub-carrier and at both edges of the frequency spectrum as typically specified in OFDM standards. (The number of additional inserted null tones in the ND scheme is counted in N_d but not in N_n).

In the following, we calculate $\rho^\dagger$ for a multipath fading channel having uncorrelated taps and power delay profile

[4] Without loss of generality, we simply set this maximum value of σ_1^2 which is the case where all data have the same average energy.

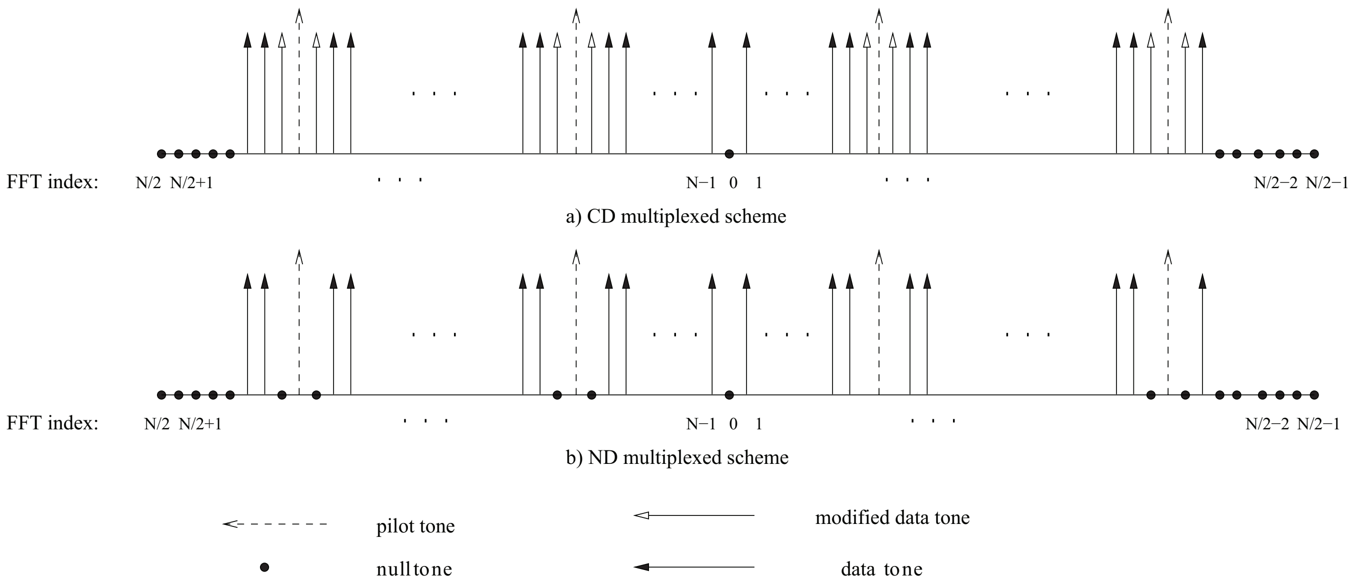

Fig. 2. Illustration of the proposed multiplexed schemes.

$\{\sigma^2_{h,n} : n = 0, \ldots, L-1\}$. For this case, we have

$$E[H^*_{m-1}H_{m+1}] = \sum_{n=0}^{L-1} \sigma^2_{h,n} e^{\frac{-j4\pi n}{N}} \tag{21}$$

which is independent of the sub-carrier index. Next, from (4), we obtain the following term

$$I^*_n I_{n+2} = \frac{2}{N^2} \frac{e^{-j2\pi/N} \ \sin^2[\pi(v+n)]}{\cos[2\pi/N] - \cos[2\pi(v+n+1)/N]} \tag{22}$$

whose phase is given by

$$\begin{aligned} \theta_{\Delta I} &= \text{angle}\{I^*_n I_{n+2}\} \\ &= \begin{cases} 0, & v = \text{integer} \\ \pi - \frac{2\pi}{N}, & Nk - 2 < v + n < Nk, \\ & v \neq \text{integer},\ k = \text{any integer} \\ \frac{-2\pi}{N}, & \text{otherwise}. \end{cases} \end{aligned} \tag{23}$$

It can be easily checked that the terms $\{I^*_{m-1-k}I_{m+1-k} : m \neq k\}$ in β_k are negligible compared to the term $I^*_{-1}I_{+1}$ (see also Fig. 1(b)). Then, from (16), (21), and (23), we obtain

$$\theta_\beta \simeq \theta_{\Delta H} + \pi - \frac{2\pi}{N} \tag{24}$$

where $\theta_{\Delta H}$ = angle$\{E[H^*_{m-1}H_{m+1}]\}$ and $|v| < 1$, $v \neq 0$ is assumed. Then (19) becomes

$$\rho^\dagger = e^{j(\frac{2\pi}{N} - \theta_{\Delta H})} \tag{25}$$

which is independent of v. Note that $\theta_{\Delta H}$ is very small for practical systems where $N \gg L$ and its effect on $\rho^\dagger$ can be neglected, i.e., $\rho^\dagger = e^{j(\frac{2\pi}{N})}$ (or $\rho^\dagger = 1$ for large N) can be used. Since the left and right ICI coefficients I_1 and I_{-1} are almost anti-symmetric, it can be intuitively understood that the left and right adjacent data tones should be almost the same, i.e., $\rho^\dagger \simeq 1$.

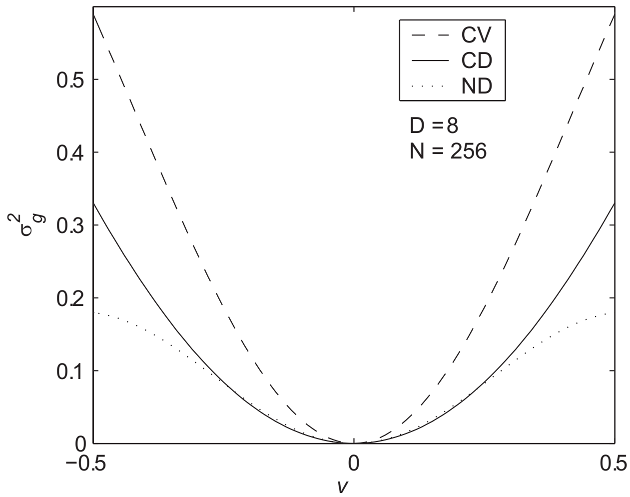

Fig. 3. The variance of the data-interference on a pilot tone for the three multiplexed schemes.

IV. Comparison of Several Schemes

The data throughputs of the CV, CD, and ND schemes are N_d/N, $(N_d - N_p)/N$, and $(N_d - 2N_p)/N$, respectively. In typical systems with $N \gg N_p$, the throughput differences are not significant. Next, we calculate σ^2_g, the ICI effect on all pilot tones, and obtain

$$\sigma^2_g = \begin{cases} \sum_{k \in \mathcal{J}_p} (\gamma_k + \frac{E_d}{N_d}\ \alpha_k), & \text{CV scheme} \\ \sum_{k \in \mathcal{J}_p} (\gamma_k + [\sigma^2_1]_{\max}\ [\alpha_k - |\beta_k|]), & \text{CD scheme} \\ \sum_{k \in \mathcal{J}_p} \gamma_k, & \text{ND scheme.} \end{cases} \tag{26}$$

Note that CV, CD, and ND schemes correspond to ($\rho = 0$, $\sigma^2_1 = \sigma^2_2 = E_d/N_d$), ($\rho = \rho^\dagger$, $\sigma^2_1 = [\sigma^2_1]_{\max}$), and ($\sigma^2_1 = 0$), respectively. Fig. 3 shows σ^2_g for all three schemes in an OFDM system with $N = 256$, $N_p = 32$, $N_n = 0$, and $N_d = 224$. Both CD and ND schemes achieve considerable

ICI reduction if compared to the CV scheme. In practice, v will be small due to prior coarse frequency synchronization. In this case, both CD and ND schemes have almost the same data interference on a pilot tone. But the CD scheme has a higher data throughput than the ND scheme. Note that the CD scheme can achieve the same data rate as the CV scheme if a larger modulation alphabet is used on data tones adjacent to pilot tones. For example, if the CV scheme uses QPSK, then the CD scheme can transmit the same data rate by using 16-QAM on data tones adjacent to pilot tones and QPSK on the remaining data tones. This modified scheme will be denoted by CD*.

In terms of complexity, there is no significant difference among the three schemes. In the CD scheme, using $\rho^{\dagger} = 1$ requires no additional complexity. After frequency-domain equalization at the receiver, the CD scheme performs averaging of the adjacent data tones and detects $N_d - N_p$ sub-carrier symbols while the CV scheme detects N_d sub-carrier symbols and the ND scheme detects $N_d - 2N_p$ sub-carrier symbols.

V. Simulation Results and Discussions

The simulation parameters are as follows. A multipath Rayleigh fading channel having $L = 16$ uncorrelated taps and an exponential power delay profile $\{\sigma_{h,n}^2 : n = 0, \ldots, L-1\}$ with a 3dB per tap decaying factor is considered. The number of sub-carriers is $N = 256$. The data-pilot-multiplexed symbol has $N_p = 32$ pilot tones, $N_n = 0$ null tone and $N_d = 244$ data tones. A packet in the simulation contains one data-pilot-multiplexed OFDM symbol followed by 5 data-only OFDM symbols using QPSK modulation. Total pilot energy and data E_b/N_0 are kept the same for all schemes. The pilot tone index-shift is $l = 0$ and the ratio of total pilot energy to total data energy within a data-pilot-multiplexed symbol is defined by PDER (Pilot-to-Data Energy Ratio). The normalized frequency offset is modeled as a uniform random variable with the range $[-0.2, 0.2]$.

In addition to CD, ND, and CV schemes, we also evaluate two other pilot-data-multiplexed schemes which use $2N_p$ pilot tones and hence have the same data throughput as the CD scheme. The first scheme (denoted by CV2) is the CV scheme with $2N_p$ (instead of N_p) pilot tones. In the second scheme (denoted by "pair"), pairs of equal energy pilot tones are located at the indices $\{mD, mD+1 : \ m = 0, \ldots, N_p - 1\}$ and the two adjacent pilot tones are the same[5]. These two adjacent pilot tones are averaged at the receiver before the estimation is carried out. We consider two sets of estimators. In the first set denoted by "Estimator-A", we use the BLUE frequency offset estimation method (Method-D) from [3] and the least-squares channel estimation [9] (after frequency offset compensation). Note that the "BLUE" estimator used in this paper is not the exact best linear unbiased estimator due to the data interference but we will refer to it as the BLUE method for convenience. It would represent an approximate BLUE by treating the data interference as additional uncorrelated noise. In the second set, denoted by "Estimator-B", we use the frequency offset estimator in [1] with a correlation distance of 128 samples and the frequency-domain least-squares channel estimator with interpolation in the sub-carrier domain.

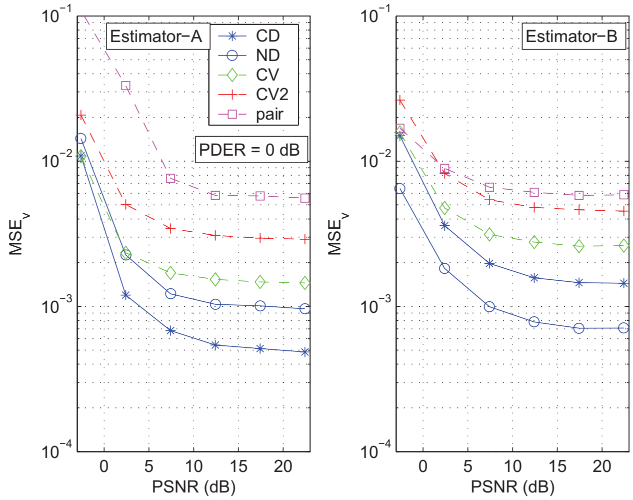

Fig. 4. Comparison of data-pilot-multiplexed schemes in terms of the MSE of normalized frequency offset estimation at PDER = 0 dB.

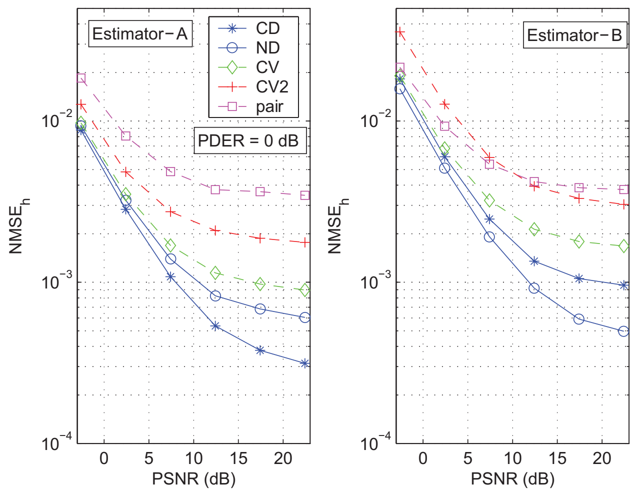

Fig. 5. Comparison of data-pilot-multiplexed schemes in terms of the normalized channel estimation MSE at PDER = 0 dB.

Figs. 4-6 present the mean-square error (MSE) of the normalized frequency offset estimation (MSE$_v$), the normalized MSE of CIR estimation (NMSE$_h$), and the BER, respectively, versus pilot signal energy to noise variance ratio (PSNR= PDER $\cdot$ DSNR where the data signal to noise ratio DSNR is given by $2\frac{E_b}{N_0}\frac{D-1}{D}$ where the factor 2 is due to the use of QPSK data symbol) with PDER = 0 dB. The corresponding results for PDER = 5 dB are shown in Figs. 7-9. The CD* scheme is also included in the BER comparison. The following remarks are in order.

1) There exist MSE$_v$ floors for all schemes due to the data interference. A larger PDER can lower the MSE floors of all schemes.
2) The proposed schemes outperform all other schemes significantly.
3) The proposed CD scheme gives better performance than the proposed ND scheme for the estimator-A while

[5]We also evaluated this scheme with adjacent pilot tones being negative of each other. Its performance is worse than the scheme with the same adjacent pilot tones.

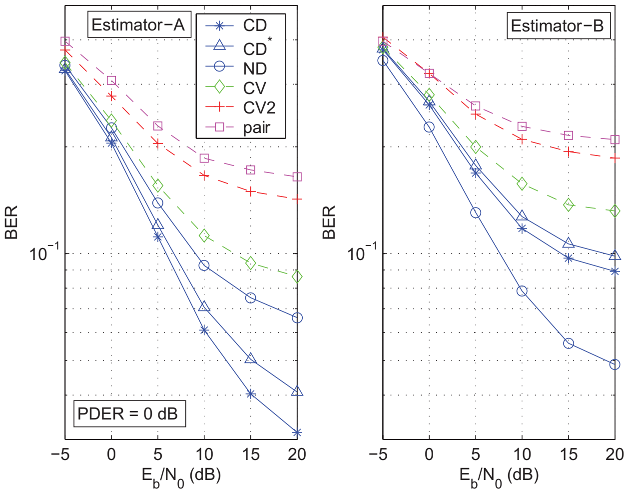

Fig. 6. Comparison of data-pilot-multiplexed schemes in terms of the uncoded BER performance at PDER = 0 dB.

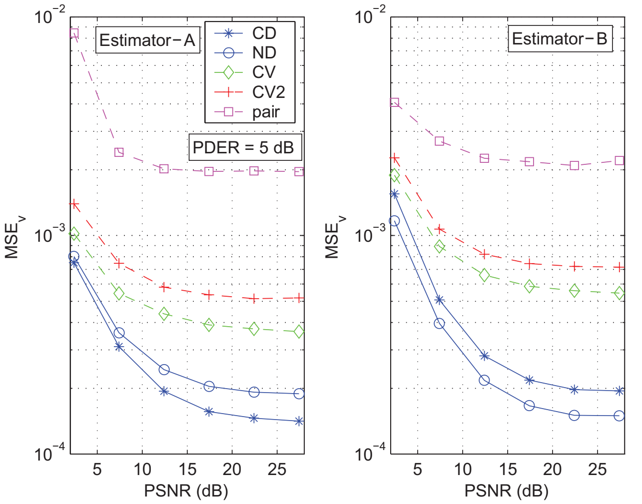

Fig. 7. Comparison of data-pilot-multiplexed schemes in terms of the MSE of normalized frequency offset estimation at PDER = 5 dB.

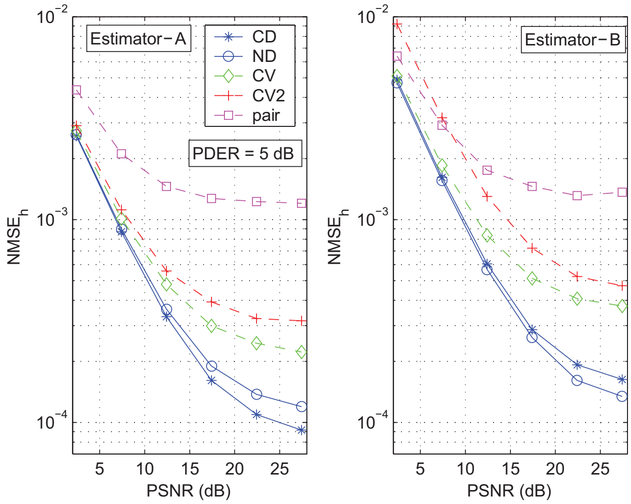

Fig. 8. Comparison of data-pilot-multiplexed schemes in terms of the normalized channel estimation MSE at PDER = 5 dB.

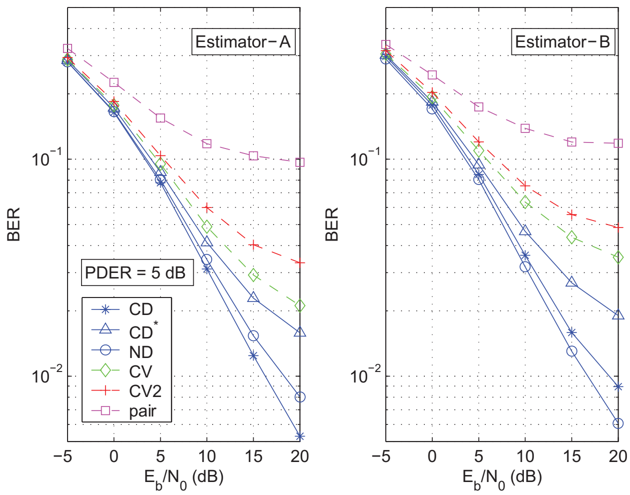

Fig. 9. Comparison of data-pilot-multiplexed schemes in terms of the uncoded BER performance at PDER = 5 dB.

the reverse holds for the estimator-B. The estimator-A performs better than the estimator-B.

4) The CD* scheme experiences a slight performance degradation (simply due to the larger error performance of 16-QAM than QPSK) if compared to the CD scheme but it still outperforms conventional schemes (CV, CV2, and pair) while having the same data rate as the CV scheme does.

The performance dependence of the proposed schemes on the estimators can be explained as follows. In the design, all interference terms are considered to negatively affect the estimation performance. However, for the CD schemes with the estimator A (B), the interference terms from the data tones adjacent to pilot yield a constructive (destructive) effect in the frequency offset estimation. The time-domain k-th sample of the adjacent data tones in the CD scheme can be given by

$$\{e^{\frac{-j2\pi k}{N}} + (\rho^\dagger)^* e^{\frac{j2\pi k}{N}}\} \sum_{l=0}^{N_p-1} S_{lD+1} e^{\frac{-j2\pi lDk}{N}} \equiv$$

$$\{e^{\frac{-j2\pi k}{N}} + (\rho^\dagger)^* e^{\frac{j2\pi k}{N}}\}\ x_k \simeq 2\cos(\frac{2\pi k}{N}) x_{k \bmod N_p} \quad (27)$$

where x_k for $k = 0, \ldots, N-1$ contains D identical parts of length N_p each, regardless of $\{S_{lD\pm1}\}$. The contribution of adjacent data tones in the CD scheme with the BLUE method (estimator-A) can be observed by inputting the term in (27) (i.e., $2\cos(\frac{2\pi k}{N})\ x_{k \bmod N_p}$ or equivalently $\cos(2\pi k/N)$)) to the BLUE method. If the channel output time-domain pilot signal is input to the BLUE method, the resulting terms before multiplying with the BLUE weighting values are all positive values. For the $\cos(2\pi k/N)$) input, the resulting terms before multiplying with the BLUE weighting values are depicted in Fig. 10 together with the BLUE weighting values. They are all positive values (except at tap 2 and 6) and hence, we can clearly observe that the adjacent data tones of the CD scheme constructively help the BLUE method, hence, resulting in a better performance for the CD scheme than σ_g^2 reflects. Inputting $\cos(2\pi k/N)$ to the frequency offset estimator of the estimator-B gives a correlation value of -64 (if the channel

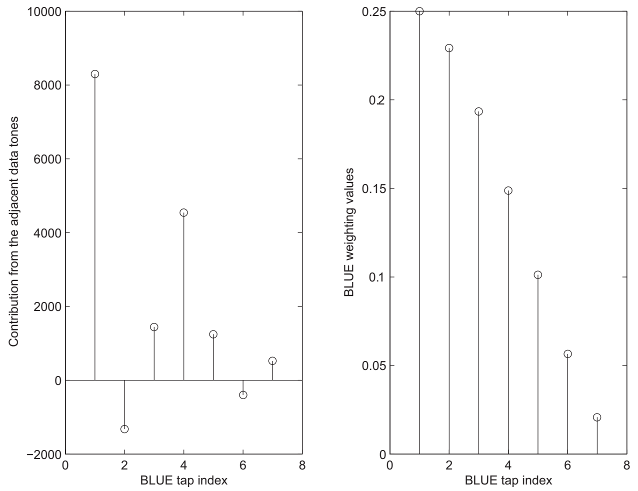

Fig. 10. Illustration of the constructive interference of the CD scheme's adjacent data tones in the BLUE frequency offset estimation.

output pilot signal is input, the corresponding value is positive) which indicates that the adjacent data tones in the CD scheme negatively affect the estimator-B.

A factor that affects the frequency offset estimation performance is the fluctuation of the received training signal energy. As long as the number of pilot tones is at least L, the time-domain identical part of the pilot signal has zero auto-correlation property which gives minimum fluctuation of the received energy. This fact translates into the minimum averaged CRB (the CRB conditioned on a particular channel realization is averaged over the random channel) of the frequency offset estimation (more details are referred to [14]). Since the numbers of pilot tones used in all schemes are at least L, there is no difference regarding the effect of received energy fluctuation on the estimation performance.

The performance differences among the proposed schemes and the reference schemes can be ascribed to three factors – the perturbation of the ICI caused by the pilot tones, the data interference on the pilot tones, and the estimator's noise suppression capability for the considered multiplexed scheme. Since the frequency offset estimation is based on the ICI caused by the pilot tones, this ICI should not be affected. The "pair" scheme performs averaging between adjacent pilot tones and hence affects the ICI induced by the pilot tones. This fact explains why its estimation performance is worse than other schemes.

Recall that we set the same total pilot energy regardless of the scheme for a fair comparison. Hence, even though CV2 and "pair" schemes have twice as many pilot tones, the pilot energy on each pilot is half of that of the CV scheme. The significant data interference terms in the estimation come from the data tones adjacent to pilot tones. Since CV2 and "pair" schemes have more pilot tones, they have more adjacent data tones which give significant interference. Consequently, CV2 and "pair" schemes are affected more by the data interference and hence are outperformed by the other schemes.

Next, consider the CD scheme and the CV2 scheme. First of all, the CD scheme has less data interference than the CV2 scheme. Even if we neglect this advantage (alternatively, if there are only pilot tones and no data), we can explain the better performance of the CD scheme as follows. Consider pilot-only case; the time-domain pilot signal of length N samples contains N/N_p identical parts in the CD scheme and $N/(2N_p)$ identical parts in the CV2 scheme. If we calculate the BLUE variance, we obtain that the pilot signal with a larger number of identical parts (whose length should be at least the number of channel taps) gives a smaller estimation variance. More details on the effect of the number of identical parts on the BLUE variance can be referred to [3]. An alternative explanation is given as follows. The estimator utilizes the time-domain periodic structure (which is due to the equi-spaced pilot tones in the frequency domain) and noise suppression is embedded in the BLUE. Since we can only suppress the noise at the non-pilot sub-carriers, we can achieve a better noise suppression if a smaller number of pilot tones ($\geq L$) are used. This fact explains why the CD scheme outperforms the CV2 scheme even at low SNR.

VI. Conclusions

In OFDM-based systems, data-pilot-multiplexed OFDM symbols are typically transmitted at a regular rate in order to track variations in channel gains and synchronization parameters. This paper derives data-pilot-multiplexed schemes which minimize data-interference (due to frequency offsets) on the pilot tones with a minimal data throughput sacrifice. This data-interference minimizing design gives a correlated data insertion scheme (CD), a null data insertion scheme (ND), and a modified CD scheme. Although this design does not guarantee minimum BER performance, our simulation results show that the proposed schemes achieve significant BER improvement over the conventional schemes (the CD and ND schemes have over 7 dB SNR advantage and the modified CD scheme has over 3 dB SNR advantage at the uncoded BER of 2×10^{-2} and PDER of 5 dB). Since the BLUE complexity is quite low, the CD scheme would be preferable over the ND scheme due to its better performance and slightly larger data throughput. Existing OFDM-based systems as well as those in standardization process have pilot-data-multiplexed OFDM symbols and hence, our proposed schemes would be useful in enhancing these systems.

References

[1] T. M. Schmidl and D. C. Cox, "Robust frequency and timing synchronization for OFDM," *IEEE Trans. Commun.*, vol. 45, no. 12, pp. 1614-1621, Dec. 1997.

[2] M. Morelli and U. Mengali, "An improved frequency offset estimator for OFDM applications," *IEEE Commun. Lett.*, vol. 3, no. 3, pp. 75-77, Mar. 1999.

[3] H. Minn, P. Tarasak, and V. K. Bhargava, "Some issues of complexity and training symbol design for OFDM frequency offset estimation methods based on BLUE principle," in *Proc. IEEE VTC (Spring)*, Apr. 2003, pp. 1288-1292.

[4] J.-J. van de Beek, M. Sandell, and P. O. Börjesson, "ML estimation of time and frequency offset in OFDM systems," *IEEE Trans. Signal Processing*, vol. 45, no. 7, pp. 1800-1805, July 1997.

[5] U. Tureli, H. Liu, and M. D. Zoltowski, "OFDM blind carrier offset estimation: ESPRIT," *IEEE Trans. Commun.*, pp. 1459-1461, Sep. 2000.

[6] P. Ciblat and E. Serpedin, "A fine blind frequency offset estimator for OFDM/OQAM systems," *IEEE Trans. Signal Processing*, pp. 291-296, Jan. 2004.

[7] Y. Zhao and S. G. Haggman, "Sensitivity to Doppler shift and carrier frequency errors in OFDM systems-the consequences and solutions," in *Proc. IEEE VTC*, Apr. 1996, pp. 1564-1568.

[8] J. Armstrong, "Analysis of new and existing methods of reducing intercarrier interference due to carrier frequency offset in OFDM," *IEEE Trans. Commun.*, pp. 365-369, Mar. 1999.
[9] H. Minn and N. Al-Dhahir, "Optimal training signals for MIMO OFDM channel estimation," *IEEE Trans. Wireless Commun.*, vol. 5, no. 5, pp. 1158-1168, May 2006.
[10] K. Sathananthan and C. Tellambura, "Probability of error calculation of OFDM systems with frequency offset," *IEEE Trans. Commun.*, vol. 49, no. 11, pp. 1884-1888, Nov. 2001.
[11] L. Rugini, P. Banelli, and S. Cacopardi, "Probability of error of OFDM systems with carrier frequency offset in frequency-selective fading channels," *IEEE Trans. Wireless Commun.*, vol. 4, no. 5, pp. 2279-2288, Sep. 2005.
[12] T. Pollet, M. Van Bladel, and M. Moeneclaey, "BER sensitivity of OFDM systems to carrier frequency offset and Wiener phase noise," *IEEE Trans. Commun.*, vol. 43, no. 2/3/4, pp. 191-193, Feb./Mar./Apr. 1995.
[13] M. Speth, S. A. Fechtel, G. Fock, and H. Meyr, "Optimum receiver design for wireless broad-band systems using OFDM-Part I," *IEEE Trans. Commun.*, vol. 47, no. 11, pp. 1668-1677, Nov. 1999.
[14] H. Minn, X. Fu, and V. K. Bhargava, "Optimal periodic training signal for frequency offset estimation in frequency-selective fading channels," *IEEE Trans. Commun.*, vol. 54, no. 6, pp. 1081-1096, June 2006.

Xiaoyu Fu (S'04) received the B.S. and M.S. degree in electrical engineering from the University of Electronic Science and Technology of China, Sichuan, China, in 1999 and 2002, respectively. He is working toward the Ph.D. degree at the University of Texas at Dallas (UTD), Dallas. Since 2003, he has been a Research Assistant with the Information and Communication Systems Laboratory at the Department of Electrical Engineering, UTD. His research interests include synchronization and channel estimation in broadband wireless communications systems.

Hlaing Minn (S'99-M'01) received his B.E. degree in Electronics from Yangon Institute of Technology, Yangon, Myanmar, in 1995, M.Eng. degree in Telecommunications from Asian Institute of Technology (AIT), Pathumthani, Thailand, in 1997 and Ph.D. degree in Electrical Engineering from the University of Victoria, Victoria, BC, Canada, in 2001.

He was with the Telecommunications Program in AIT as a laboratory supervisor during 1998. He was a research assistant from 1999 to 2001 and a post-doctoral research fellow during 2002 in the Department of Electrical and Computer Engineering at the University of Victoria. Since September 2002, he has been with the Erik Jonsson School of Engineering and Computer Science, the University of Texas at Dallas, USA, as an Assistant Professor. His research interests include wireless communications, statistical signal processing, error control, detection, estimation, synchronization, signal design, and cross-layer design. He is an Editor for the IEEE TRANSACTIONS ON COMMUNICATIONS.